

---

This is an electronic reprint of the original article.  
This reprint may differ from the original in pagination and typographic detail.

Jayathurathnage, Prasad Kumara Sampath; Dang, Xiaojie; Simovski, Constantin; Tretyakov, Sergei

## Self-tuning Omnidirectional Wireless Power Transfer using Double Toroidal Helix Coils

*Published in:*  
IEEE Transactions on Industrial Electronics

*DOI:*  
[10.1109/TIE.2021.3097663](https://doi.org/10.1109/TIE.2021.3097663)

Published: 01/07/2022

*Document Version*  
Peer-reviewed accepted author manuscript, also known as Final accepted manuscript or Post-print

*Please cite the original version:*  
Jayathurathnage, P. K. S., Dang, X., Simovski, C., & Tretyakov, S. (2022). Self-tuning Omnidirectional Wireless Power Transfer using Double Toroidal Helix Coils. *IEEE Transactions on Industrial Electronics*, 69(7), 6828-6837. <https://doi.org/10.1109/TIE.2021.3097663>

---

This material is protected by copyright and other intellectual property rights, and duplication or sale of all or part of any of the repository collections is not permitted, except that material may be duplicated by you for your research use or educational purposes in electronic or print form. You must obtain permission for any other use. Electronic or print copies may not be offered, whether for sale or otherwise to anyone who is not an authorised user.

# Self-tuning Omnidirectional Wireless Power Transfer using Double Toroidal Helix Coils

Prasad Jayathurathnage, Xiaojie Dang, Constantin R. Simovski, and Sergei A. Tretyakov

**Abstract**—We suggest and study a novel omnidirectional wireless power transfer (WPT) system based on unusual double toroidal helix coils. The suggested antenna is a double-helix coil wound around a torus. It creates two mutually orthogonal magnetic fields. One is toroidal and confined inside the torus, another one is poloidal and is distributed outside it. The intensities of these two fields can be independently tuned via the geometry of the turns. The coupling coefficients are tailored to ensure high efficiency regardless of the receiver position and orientation, without active circuitry for tuning or control. This topology provides self-tuning functionality which is achieved when the coupling between the transmitter and receiver is minimized while the coupling in the pairs transmitter-repeater and repeater-receiver is strong. The system consists of three transmitter-repeater pairs orthogonal to each other, ensuring omnidirectional functionality. Experimental results confirm self-tunability and high efficiency for any position and orientation of receivers. The proposed double-helix antenna is applicable to different WPT applications where the coupling/decoupling between coils can be freely controlled.

**Index Terms**—Wireless power transfer, omnidirectional power, toroidal helix coil, toroidal field, poloidal field.

## I. INTRODUCTION

WIRELESS power transfer (WPT) is increasingly becoming a popular technique for diverse applications including electric vehicle charging, implantable medical devices, robotic systems, wearable electronics, and sensor networks [1]–[4]. The transmission efficiency of conventional WPT systems is sensitive to the alignment of the transmitter (Tx) coil and the receiver (Rx) coil, which limits the coverage area. Recently, omnidirectional WPT in three-dimensional (3D) space have been introduced to enable ubiquitous wireless charging [2], [5]–[12]. For example, such ubiquitous WPT solution would enable wireless charging of multiple consumer electronics devices (e.g. laptops, mobile phones, kitchen appliances) regardless of their location in an indoor environment (see a conceptual illustration in Fig. 1). In addition, wireless charging of multiple biomedical implants such as micro-implants and micro-sensors requires such omnidirectional WPT method. Another important application of omnidirectional WPT devices is charging of multiple sensors. For instance, charging of agricultural sensors in a large field requires tedious manual intervention. This problem can be solved by using an omnidirectional WPT system, where a WPT transmitter can be moved along the field to charge all the sensors without interfering with them. For all these examples, a prime requirement is robust and efficient power transfer in 3D space regardless of receiver orientation and without the

need for complex tuning or control circuits. In particular, high-efficiency operation at different receiver orientations is highly demanded for these applications.

There have been different proposals to enable efficient omnidirectional WPT [2], [5]–[12]. Primarily, there are two types of omnidirectional WPT systems: 1. a single 3D Tx coil with multiple windings in different directions; and 2. multiple Tx coils at different orientations. In the first approach, it is possible to achieve efficient power transfer for selected receiver positions in 3D space, however, inevitably, there are several *blind* areas, where the power transfer is not effective [13], [14]. This is because magnetic flux generated by one winding cancels out with the flux generated by another one for certain receiver positions. In fact, for a fixed input current, the combination of magnetic fields induced by multiple windings is always directional. Therefore, using single Tx based solutions, it is impossible to realize truly omnidirectional covering of charging. Although the use of multiple Tx coils in orthogonal directions is a viable option to achieve effective WPT in omnidirectional space, it requires detection of the receiver position and control of the power flow in different Tx's using complex control methods. For example, papers [6] and [15] employ additional feedback from the Rx-side for the receiver detection and a controller to control the coil currents to maintain efficient power transfer in omnidirectional space. However, additional circuits for position detection and current control make the system complex and less flexible.

In order to solve these problems, in Ref. [10] the au-

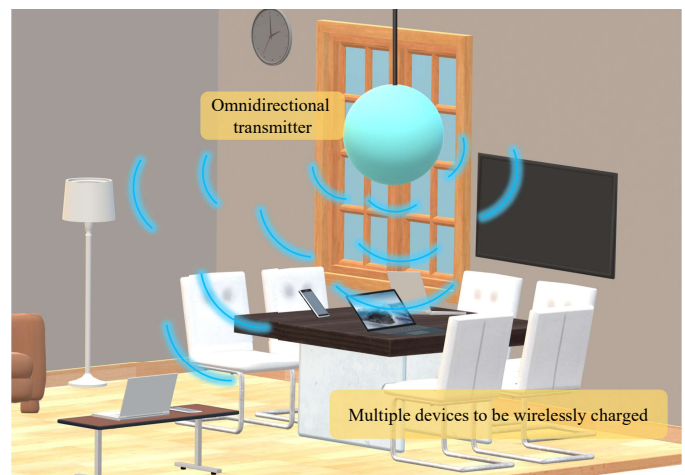


Fig. 1. A conceptual illustration of an omnidirectional WPT for consumer electronic devices in an indoor environment.

thors proposed a 3D omnidirectional WPT system with three orthogonal transmitter-repeater (Tx-Rp) pairs forming three independent *power channels*. That system enables self-tuning of the power flow from each Tx without having any feedback control system for detecting and tracking the receiver position. The power flow in each *power channel* is self-tuned being proportional to the mutual coupling between the repeater (Rp) and receiver (Rx) of this power channel. The self-tuning feature means that the current in each Tx coil is inherently proportional to the mutual inductance between the respective repeater and receiver without any control. This means that the optimal current modulation condition in [5] can readily be achieved without complex current control methods. Therefore, the self-tuning feature ensures that the power extracted by each Tx coil is self-tuning based on the receiver position, i.e., if the receiver is closer to a particular Tx-Rp pair (having higher Rp-Rx coupling), the power extracted by that Tx is higher than the power extracted by a Tx far away from the Rx (having lower Rp-Rx coupling). In order to approach the ideal self-tuning, the mutual coupling in the Tx-Rp and Rp-Rx coil pairs should be strong, while the mutual coupling between Tx and Rx coils should be negligibly small [10]. However, when both Tx and Rp are physically located in the transmitting sub-system of the WPT system, and there is no design freedom to tune the coupling coefficients properly. For classical spiral coils this is a restriction which limits the self-tuning functionality.

A similar functionality and efficiency as in Ref. [10] were demonstrated also in works [16], [17], where higher-order compensation circuits were used to engineer current-source driven Tx coils. In papers [14], [18] the so-called LCC-S WPT systems were introduced which manifested both high efficiency and high isotropy of the power transfer. However, the additional elements in the compensation network usually require the use of magnetic materials. These approaches severely limit the working frequency. With the emerging WPT applications in wearable electronics and internet-of-things, it is necessary to design WPT systems capable to operate at much higher frequencies [19].

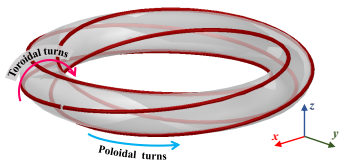


Fig. 2. The proposed toroidal helix coil shape and an illustration of toroidal turns and poloidal turns.

In this paper, we propose novel toroidal-helix coils for efficient self-tuning omnidirectional WPT systems. These coils have two winding directions: poloidal and toroidal, as depicted in Fig. 2. As we will describe in the following section, we design the Tx coil to generate mainly toroidal field and the Rx coil to generate magnetic fields of predominantly poloidal direction. On the other hand, the Rp coil is designed so that to receive and radiate both poloidal and toroidal fields, as shown in Fig. 3. Therefore, the Tx-Rp coupling and Rp-Rx coupling are realized mainly via the toroidal and poloidal fields, re-

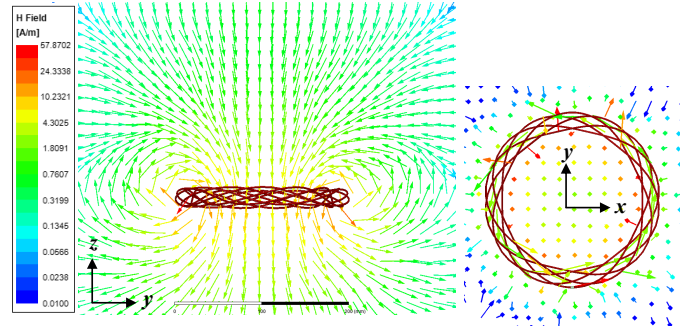


Fig. 3. Magnetic field distribution of the proposed toroidal helix coil.

spectively. Furthermore, the direct coupling between Tx and Rx is very small because their dominant fields are orthogonal to each other. Therefore, this inherent feature results in the fact that the coupling of Rp-Tx is far stronger than that of Tx-Rx, which is the critical requirement for self-tuning WPT, as is shown in [10]. The proposed coil structure also acts as current-source driven Rp coil, therefore, can also be used as an alternative for higher-order compensation networks without creating any limitation on the working frequency.

The paper is organized as follows. The equivalent circuit analysis is presented in Section II, which explains the requirement of having low coupling between Tx and Rx compared to that between Rp and Rx. Next, the proposed toroidal helix coil is introduced in Section III with a design example. Finally, the proposed concept is experimentally verified in Section IV, followed by conclusions.

## II. THEORETICAL ANALYSIS

### A. The Equivalent Circuit

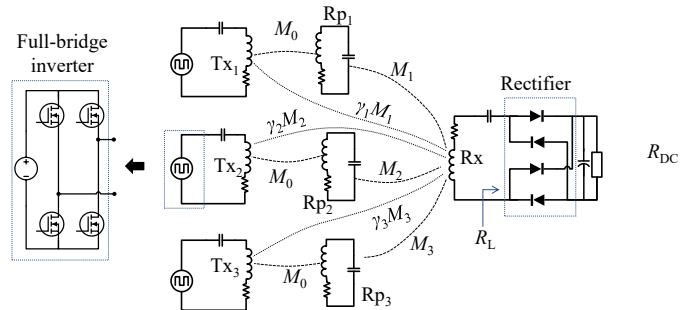


Fig. 4. The equivalent circuit of the proposed WPT system with three Tx-Rp pairs and one Rx.

We start our discussion by analysing self-tuning omnidirectional WPT systems using the equivalent circuit method and highlight the advantages of the proposed coil shapes. The proposed omnidirectional WPT system consists of three Tx-Rp coil pairs (i.e.,  $Tx_{1,2,3}$ , and  $Rp_{1,2,3}$ ) orthogonal to each other. The equivalent circuit of the proposed WPT system is shown in Fig. 4. Because the resonant network has a high quality factor, the fundamental-harmonic approximation is used to analyse the system characteristics. The Rp and Rx coils are tuned to the working frequency  $\omega_0$  by using series capacitors, while

the Tx coils are tuned to exhibit a non-zero reactance  $X_t$  at the working frequency, so that the Tx resonant frequency is smaller than the working frequency  $\omega_0$ . The Tx coils are connected to high-frequency sources, for example, to full-bridge converters, as illustrated in Fig. 4. As the three Tx-Rp pairs are orthogonal to each other, the cross couplings between different pairs are negligibly small. Considering the fundamental harmonic, the system equation of the equivalent circuit can be written as

$$\begin{bmatrix} \vec{V}_{\text{Tx}} \\ \vec{0} \\ 0 \end{bmatrix} = \begin{bmatrix} R_{\text{Tx}} + jX_t & j\omega_0 M_0 & j\omega_0 \vec{\Gamma} \\ j\omega_0 M_0 & R_{\text{Rp}} & j\omega_0 \vec{M} \\ j\omega_0 \vec{\Gamma}^T & j\omega_0 \vec{M}^T & R_L + R_{\text{Rx}} \end{bmatrix} \begin{bmatrix} \vec{I}_{\text{Tx}} \\ \vec{I}_{\text{Rp}} \\ I_{\text{Rx}} \end{bmatrix}, \quad (1)$$

where  $\vec{V}_{\text{Tx}} = [V_s \ V_s \ V_s]^T$  denote the three identical source voltages,  $\vec{I}_{\text{Tx}} = [I_{\text{Tx}1} \ I_{\text{Tx}2} \ I_{\text{Tx}3}]^T$ ,  $\vec{I}_{\text{Rp}} = [I_{\text{Rp}1} \ I_{\text{Rp}2} \ I_{\text{Rp}3}]^T$ , and  $I_{\text{Rx}}$  denote the currents in the TxS, Rps, and RxS.  $R_{\text{Tx}}$ ,  $R_{\text{Rp}}$ , and  $R_{\text{Rx}}$  represent parasitic resistances of Tx, Rp, and Rx coils, respectively.  $M_0$  is the mutual inductance between the transmitter and the repeater belonging to the same channel,  $\vec{M} = [M_1 \ M_2 \ M_3]^T$  denotes the mutual inductance between each repeater coil and the receiver coil, and  $\vec{\Gamma} = [\gamma_1 M_1 \ \gamma_2 M_2 \ \gamma_3 M_3]^T$  denotes the mutual inductance between each transmitter coil and the receiver coil. Finally,  $\gamma_1$ ,  $\gamma_2$  and  $\gamma_3$  represent the ratio of mutual inductances between Tx-Rx and Rp-Rx for each channel.

The effects of parasitic resistances can be neglected for the calculation of the input impedance when  $R_L \gg R_{\text{Rx}}$  and  $\omega_0 M_i \gg R_{\text{Tx}}$ ,  $R_{\text{Rp}}$ . These assumptions always hold in practical applications: the parasitic resistances of coils are small compared to the load resistance, and coupling between the coils dominates over the parasitic coil resistance. Therefore, with the assumption of  $R_{\text{Tx}} = R_{\text{Rp}} = R_{\text{Rx}} \approx 0$ , the input reactances  $X_{\text{in},i}$  and input resistances  $X_{\text{in},i}$  seen from the  $i^{\text{th}}$  transmitter are

$$X_{\text{in},i} = \frac{X_t \vec{M} \cdot \vec{M} - 2\omega_0 M_0 \vec{\Gamma} \cdot \vec{M}}{M_{\text{sum}} M_i}, \quad (2)$$

$$R_{\text{in},i} = \frac{M_0^2 R_L}{M_i M_{\text{sum}}}, \quad (3)$$

where  $M_{\text{sum}} = M_1 + M_2 + M_3$ . We can easily make the input reactances  $X_{\text{in},i}$  to be zero by choosing

$$X_t = \frac{2\omega_0 M_0 \vec{\Gamma} \cdot \vec{M}}{\vec{M} \cdot \vec{M}} \quad (4)$$

to ensure operation at resonance for each transmitter source. Note that the input impedance of the WPT system will be equal to  $R_{\text{in},i}$ . Under the above condition, the currents inside  $i^{\text{th}}$  transmitter ( $I_{\text{Tx},i}$ ), repeater ( $I_{\text{Rp},i}$ ), and the receiver ( $I_{\text{Rx}}$ ) can be expressed as

$$I_{\text{Tx},i} = \frac{M_{\text{sum}} V_s}{M_0^2 R_L} M_i, \quad (5)$$

$$I_{\text{Rp},i} = -j \frac{V_s}{\omega_0 M_0} - \frac{M_{\text{sum}} \left( 2\vec{\Gamma} \cdot \vec{M} - \vec{M} \cdot \vec{M} \gamma_i \right) V_s}{\vec{M} \cdot \vec{M} M_0^2 R_L} M_i, \quad (6)$$

$$I_{\text{Rx}} = -\frac{M_{\text{sum}}}{M_0} \frac{V_s}{R_L}, \quad (7)$$

We note that the Tx currents are proportional to  $\vec{M}$ , which is analogous to the optimal Tx currents in *directional* WPT devices [15]. That is, the current in the corresponding Tx coil is suppressed when the coupling between the receiver and the particular repeater is very small. This means that the power transfer contribution from a particular Tx is automatically adjusted proportional to the mutual inductance between the receiver and its repeater. This is an essential and desired criterion for self-tuning high-efficiency omnidirectional WPT systems. This self-tuning capability is also reflected in the fact that the Rx current  $I_{\text{Rx}}$  is proportional to  $M_{\text{sum}}$ , and stable output power can be achieved as long as the total coupling inductance  $M_{\text{sum}}$  between the repeaters and receiver is stable. Moreover, we notice that the real part of the Rp current  $\vec{I}_{\text{Rp}}$  does not contribute to transferred power. Therefore, we should minimize the real part of  $\vec{I}_{\text{Rp}}$  to improve the efficiency. To this end, the coupling ratios  $\vec{\gamma}$  should be minimised. We further elaborate this requirement in the following subsection by analysing the performance characteristics.

## B. WPT Performance

The output power and efficiency of the WPT system are calculated using (5)–(7). The output power  $P_{\text{out}}$  can be calculated as

$$P_{\text{out}} = |I_{\text{Rx}}|^2 R_L = \left( \frac{M_{\text{sum}}}{M_0} \right)^2 \frac{V_s^2}{R_L}. \quad (8)$$

We can observe from Eq. (8) that the output power is proportional to  $M_{\text{sum}}^2$ , which is comparable to the  $P_{\text{out}}$  profile in the amplitudes-controlled *directional* WPT systems [6], [15]. Therefore, to obtain a stable output power, we require a stable  $M_{\text{sum}}^2$ . However, as explained in Section III, if we use circular orthogonal coils (either the proposed structure or classical coil types),  $M_{\text{sum}}^2$  may not be always stable when the Rx moves around the 3D Tx. Next, the power efficiency can be found as

$$\eta = \frac{1}{1 + \xi_{\text{Tx}} + \xi_{\text{Rp}} + \xi_{\text{Rx}}}, \quad (9)$$

$$\text{where } \xi_{\text{Tx}} = \frac{\vec{M} \cdot \vec{M} R_{\text{Tx}}}{M_0^2 R_L}, \quad \xi_{\text{Rx}} = \frac{R_{\text{Rx}}}{R_L},$$

$$\xi_{\text{Rp}} = \frac{3R_{\text{Rp}} R_L}{\omega^2 M_{\text{sum}}^2} + \frac{\vec{\Gamma} \cdot \vec{\Gamma} R_{\text{Rp}}}{M_0^2 R_L}.$$

The values of  $\xi_{\text{Tx}}$ ,  $\xi_{\text{Rp}}$ , and  $\xi_{\text{Rx}}$  represent parasitic resistive losses in TxS, Rps, and Rx relative to the output power, respectively. In practical applications, coil resistances  $R_{\text{Tx}}$  and  $R_{\text{Rx}}$  are much smaller than the load resistance. This leads to

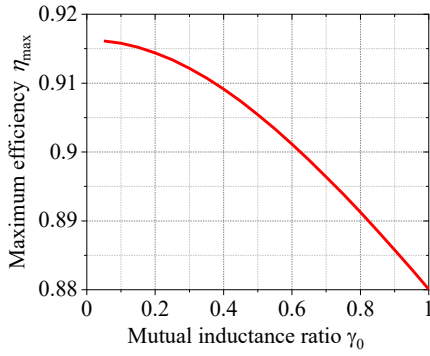


Fig. 5. The maximum efficiency given by Eq. (11) with respect to the ratio  $\gamma_0$ . (Numerical values are chosen from the experimental study presented in this paper:  $M_0 = 10 \mu\text{H}$ ,  $f_0 = \omega_0/2\pi = 600 \text{ kHz}$ ,  $M_{\text{sum}} = 12.6 \mu\text{H}$ ,  $R_{\text{Tx}} = 220 \text{ m}\Omega$ ,  $R_{\text{Rp}} = 2 \Omega$  and  $R_{\text{Rx}} = 680 \text{ m}\Omega$ .)

the fact that losses within Rx  $\xi_{\text{Rx}}$  and Tx  $\xi_{\text{Tx}}$  are very small if  $\vec{M} \cdot \vec{M}$  is comparable to  $M_0^2$ . Therefore, the most prominent losses are from the Rps. To improve efficiency,  $\gamma_1$ ,  $\gamma_2$  and  $\gamma_3$  must be kept as low as possible while maintaining high  $M_{\text{sum}}^2$ . Since all the Tx-Rp pairs are identical, it is reasonable to assume that  $\gamma_1 = \gamma_2 = \gamma_3 = \gamma_0$ .

Furthermore, we can find the optimal load resistance that corresponds to the maximum efficiency,

$$R_L = \frac{\omega_0 M_{\text{sum}}}{\sqrt{3R_{\text{Rp}}M_0}} \sqrt{M_0^2 R_{\text{Rx}} + (R_{\text{Tx}} + R_{\text{Rp}}\gamma_0^2)\vec{M} \cdot \vec{M}}, \quad (10)$$

and the maximum efficiency  $\eta_{\text{max}}$  when the load resistance is at its optimal value can be derived as

$$\eta_{\text{max}} = \frac{1}{1 + \frac{2\sqrt{3R_{\text{Rp}}(M_0^2 R_{\text{Rx}} + \vec{M} \cdot \vec{M}(R_{\text{Tx}} + \gamma_0^2 R_{\text{Rp}}))}}{\omega_0 M_0 M_{\text{sum}}}}. \quad (11)$$

From this equation we can see that the maximum efficiency is limited by the value of  $\gamma_0$ , which needs to be minimized to increase the maximum efficiency. We further elaborate this with a numerical example, considering variation of the maximum efficiency as a function of the ratio  $\gamma_0$ , shown in Fig. 5. We can see that reducing  $\gamma_0$  from 1 to 0.05 results in an efficiency increase by  $\sim 4\%$ . Therefore, it is now evident from the above analysis that low  $\gamma_0$  is the key requirement for high efficiency and self-tunability, meaning that the mutual coupling between the Tx-Rx pairs should be much lower than the mutual coupling between the Rp-Rx pairs in the same power channel.

### III. THE PROPOSED WPT SYSTEM

#### A. Toroidal Helix

From the above analysis, it is apparent that we need to enhance the mutual coupling in the coil pairs Rp-Rx and Tx-Rp i.e., ensure high values of  $M_0$  and  $\vec{M}$ , while minimizing the mutual coupling between Tx and Rx i.e., minimize  $\gamma_0$ . These conditions are not easily achievable with conventional coil designs. For example, there have been several proposals to

achieve this functionality by restricting the geometric positions of Tx and Rp coils [20] or by using Tx with a smaller diameter compared to Rp and Rx [10]. As we have already discussed, these solutions are not ideal, since they limit the operational frequencies of WPT systems.

In order to ensure that the transmitter coil strongly couples to the repeater, but, at the same time, produces negligible flux at the position of the receiving coil, we need to find a coil whose flux is localized in a certain volume. One possible topology is a tightly wound toroidal coil, because in this case nearly all the magnetic flux of the coil is concentrated inside the torus volume. In order to maximize coupling between the transmitter and repeater, we propose to wind the repeater coil over the same torus. In this case, both transmitter and repeater coils share the same toroidal flux, which is nearly equal to the flux created by the transmitter coil. Thus, the coupling between the transmitter and repeater is always strong enough. But, on the other hand, the repeater coil should couple to the receiver, which is at a different position. To ensure this coupling, we use a repeater coil with a relatively small number of turns around the toroidal core. Such coil still picks up the full flux of the transmitting coil, but at the same time it creates strong flux in the direction orthogonal to the torus plane, similarly to a usual loop. This flux extends far from the torus location and can be effectively picked up by the receiving coil.

Based on these ideas, in this paper, we suggest a toroidal double-helix coil which is compatible with the main requirements for effective, self-tunable omnidirectional operation of the WPT system. The proposed coil shape is shown in Fig. 2. Here, the winding is wrapped around a torus where it creates two kinds of electromagnetic fields: turns going along the torus that generate magnetic field in the poloidal direction are termed as poloidal turns, and turns going around the torus core that generate fields in the toroidal direction are termed as toroidal turns. The number of toroidal turns per single poloidal turn is denoted as  $N_t$  while the number of poloidal turns is denoted as  $N_p$ . We use subscripts -tx, -rp, and -rx to denote the specifications for the Tx, Rp and Rx coils, respectively.

For the Tx coil, there is only one single poloidal turn ( $N_{\text{p-tx}} = 1$ ) but a substantial number of toroidal turns ( $N_{\text{t-tx}}$ ). Therefore, the Tx coil predominantly creates a toroidal field confined inside the torus, and the poloidal field is only generated from a single poloidal turn, which can be neglected. For the Rp coil, we use the same torus core as the Tx/Rp coil, and chose substantial numbers of both  $N_{\text{t-rp}}$  and  $N_{\text{p-rp}}$ , so that this coil creates both toroidal and poloidal fields.

Finally, for the Rx coil, any shape of a receiver coil can be chosen as long as the coil is resonant and suitable to receive poloidal magnetic fields. For example, a classical multi-turn spiral-shaped coil or a similar double-helix coil with a small number of toroidal turns can be used as the Rx coil. However, the proposed double helix coil can accommodate more turns in the same volume as compared to classical spiral coils. Therefore, based on structural feasibility, we chose  $N_{\text{t-rx}} = 1$  and a substantial number for  $N_{\text{p-rx}}$  so that the Rx coil predominantly couples with the poloidal field. In this way, the coupling between Tx and Rp is through the toroidal field, while the coupling between the Rp and Rx is through the

poloidal field. Therefore, we ensure substantially high values for  $M_0$ , and  $\vec{M}$ . At the same time, direct coupling between Tx and Rx is minimal because their prevailing fields do not couple to each other, resulting in a low value for  $\gamma_0$ . Next, we present a numerical case study together with optimization of the coil parameters.

### B. Design Example and Simulation Results

In this section, we describe the optimized design of a Tx-Rp pair and present some simulation results. To this end, we select the coil outer diameter to be 200 mm and all the coils are wound on a torus core with the 20 mm diameter. The mutual inductances between the Tx, Rp, and Rx coils are analysed using a three-coil setup where the Tx coils and Rp coil are wound on the same torus core placed in the  $xoy$ -plane while the Rx is placed in parallel to the Tx-Rp with a  $z$ -direction displacement, as illustrated in Fig. 2. Note that the proposed self-tuning concept and the coil structure are generally applicable regardless of the operating frequency. In order to achieve a high coil quality factor, we have chosen the operating frequency to be around 600 kHz. The simulations are carried out using the ANSYS simulation tool, and the analytical calculations are made by approximating all the turns are elementary circular loops, similarly to [21]. For the analysis of Tx and Rp specifications, we keep the Rx coil parameters fixed with  $N_{p-rx} = 20$  and  $N_{t-rx} = 1$ .

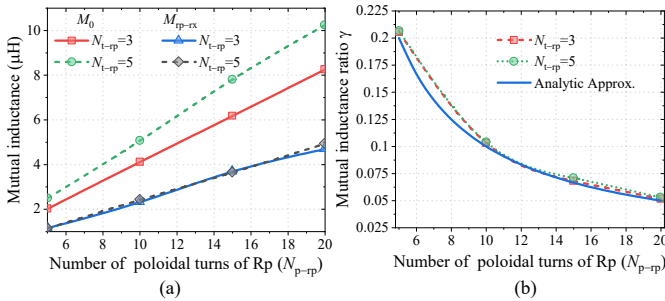


Fig. 6. (a) Variation of mutual inductances  $M_0$  and  $M$  versus the number of poloidal turns for the proposed WPT system. (b) Variation of the mutual inductance ratio  $\gamma$  with the number of poloidal turns for the proposed WPT system.

First, we discuss the effect of the number of poloidal turns of the repeater  $N_{p-rp}$  on the mutual inductances  $M_0$  and  $M$  and the mutual inductance ratio  $\gamma$ . Here,  $\gamma$  represents one of the values of  $\gamma_{1,2,3}$ , since we consider one pair of Tx-Rp coils. We can see from the results in Fig. 6 (a) that both  $M_0$  and  $M$  increase with the increase of  $N_{p-rp}$  because the coupling strengths of both poloidal field and toroidal field components are enhanced. On the other hand, the increase of  $N_{t-rp}$  helps us to enhance the toroidal coupling strength between the Tx and Rp; however, it does not affect the poloidal coupling between the Rp and Rx. Therefore, in terms of coupling enhancement, the increase of poloidal turns of Rp  $N_{p-rp}$  is more effective compared to the increase of the number of its toroidal turns.

In addition, we can approximate  $\gamma$  as the ratio of the numbers of poloidal turns of the Tx and Rp coils, i.e., as

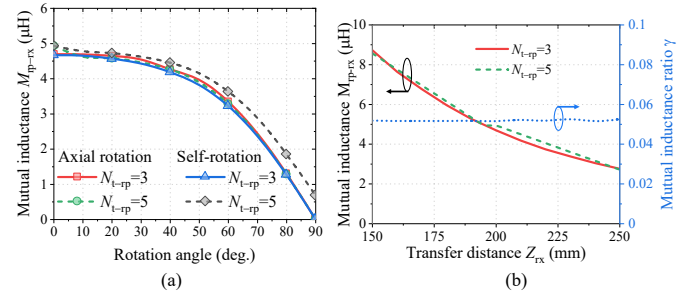


Fig. 7. (a) Variation of mutual inductance  $M$  versus rotating angle of axial rotation and self-rotation of receiver. (b) Variation of mutual inductance  $M$  and mutual inductance ratio  $\gamma$  versus the transfer distance to the receiver.

$1/N_{p-rp}$ . Therefore, the ratio  $\gamma$  decreases with the increase of  $N_{p-rp}$ . The variation of  $\gamma$  with respect to  $N_{p-rp}$  is illustrated in Fig. 6 (b), and we notice that the simulation results agree well with the analytical approximation. Next, mutual coupling strength variations against receiver positions and orientations including rotation around  $x$ -axis, self-rotation of the Rx around its principal axis, and the distance between the Rp and Rx are shown in Fig. 7 for different values of  $N_{t-rp}$ . We can clearly see from Fig. 7 that coupling between the Rp and Rx is mostly independent of  $N_{t-rp}$ . In addition, we observe that the mutual inductance ratio  $\gamma$  does not change with the receiver position, which verifies the assumption of  $\gamma_1 = \gamma_2 = \gamma_3 = \gamma_0$ .

It is obvious from the above analysis that the use of a higher number of poloidal turns of repeater is effective for the increase of  $M_0$  and  $N_{p-rp}$ , as well as for decrease of  $\gamma_0$ . The upper limit for  $N_{p-rp}$  is determined by the physical size of the torus. There should be a sufficient gap between the turns close to the wire diameter to avoid unwanted high proximity-effect losses [22]. Therefore, based on the above analysis, we chose  $N_{p-rp} = 20$  and  $N_{t-rp} = 3$ .

Next, we need to increase the number of toroidal turns of Tx  $N_{t-tx}$  to create a strong toroidal field, which helps to enhance the mutual inductance  $M_0$ . However, an increase of  $N_{t-tx}$  leads to an increase in the Tx coil resistance. Therefore, increase of  $N_{p-rp}$  is more effective for increasing  $M_0$  provided that the number  $N_{t-tx}$  is substantial. Therefore, we set  $N_{t-tx} = 75$  to ensure sufficient coupling between the Tx and Rp.

### C. The System Description

The key component of the proposed WPT system is the complex coil pictured in Fig. 8. It consists of three double-helix transmitter-repeater pairs. The three pairs are placed in an orthogonal way and form three independent *power channels*. The coil pairs Tx1-Rp1 and Tx2-Rp2 are placed in the planes perpendicular to the  $xoy$ -plane at the  $\phi = 315^\circ$  and  $\phi = 45^\circ$ , with respect to the  $xoz$ -plane, while Tx3-Rp3 is placed in the  $xoy$ -plane. Note that the orientation of the Tx coils is used only as a reference for the measurement. We choose Tx and Rp coils with the outer radius of 100 mm and the inner radius of 10 mm. Based on the analysis in the previous section, the numbers of turns  $N_{t-tx}$ ,  $N_{p-rp}$ , and  $N_{t-rp}$  are set to 75, 20, and 3, respectively.

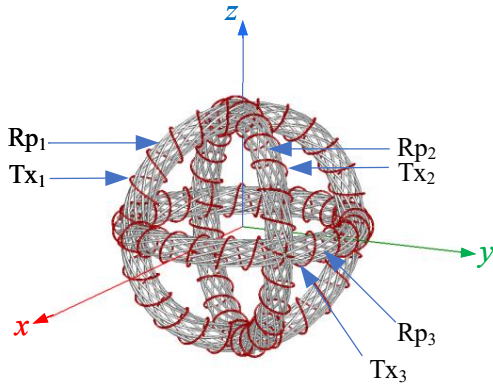


Fig. 8. Illustration of the proposed toroidal helix-shaped Tx-Rp arrangement.

Fig. 9 shows the mutual inductances  $M$  between the repeater coils and the receiver in the three-dimensional space when the receiver is placed 200 mm away from the center of the omnidirectional transmitter, with the normal unit vector pointing to the receiver from the coordinate origin. The mutual inductance is at maximum when the plane of the receiver coil is parallel to the plane of the repeater. The mutual inductance decreases to zero when two coils are orthogonal to each other. Three orthogonal repeaters make the 3D graphs of the mutual inductance orthogonal. The maximum value of the summation of the mutual inductances  $M_{\text{sum}}$  lies in the diagonal direction of eight quadrants in the planes  $xoz$  and  $yoze$ . In Fig. 9, we highlight five specific lines (Cases A – E) to show the corresponding receiver trajectories that we used during the experimental study.

Based on Eq. (8), the output power for this 3D-transmitter system is proportional to  $M_{\text{sum}}^2$ , as shown in Fig. 10(b). Therefore, if the input voltage is fixed, the output power has a similar profile as  $M_{\text{sum}}^2$ . The fluctuations in the output power (or  $M_{\text{sum}}^2$ ) are inevitable for all omnidirectional WPT schemes. Nevertheless, due to the self-tuning capability in the proposed WPT system, the input current ( $|I_{\text{Tx}1}| + |I_{\text{Tx}2}| + |I_{\text{Tx}3}|$ ) is proportional to  $M_{\text{sum}}$ , resulting in the fact that the input power is also proportional to  $M_{\text{sum}}^2$ . Therefore, efficiency is high and

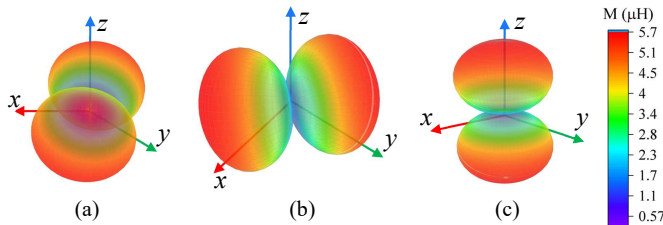


Fig. 9. The mutual inductance  $M$  between Rp1, Rp2, Rp3, and Rx when Rx rotates at the distance of 200 mm from the center of the repeaters. (a)  $M_1$  (the mutual inductance between Rp1 and Rx), (b)  $M_2$  (the mutual inductance between Rp2 and Rx), (c)  $M_3$  (the mutual inductance between Rp3 and Rx)

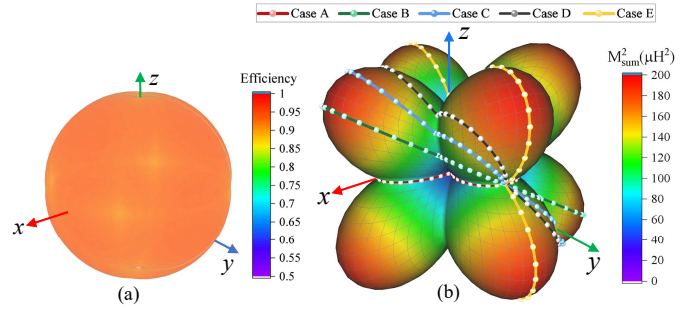


Fig. 10. (a) The efficiency of the proposed WPT system when Rx rotates at the distance of 200 mm from the center of 3D transmitters. (b)  $M_{\text{sum}}^2$  of the proposed WPT system when Rx rotates at the distance of 200 mm from the center of the 3D transmitters. Case A (red line) in  $xoy$ -Plane; Case B (green line) - elevation angle  $30^\circ$  with  $xoy$ -Plane; Case C (blue line) - elevation angle  $45^\circ$  with  $xoy$ -Plane; Case D (black line) - elevation angle  $56^\circ$  with  $xoy$ -Plane; Case E (yellow line) - elevation angle  $90^\circ$  with  $xoy$ -Plane.

stable for all the receiver positions, as shown in Fig. 10(a).

In order to clarify the effect of receiver's rotational trace on the contour of  $M_{\text{sum}}^2$ , we choose five different rotational traces of the receiver (see Fig. 10(b)), i.e., Case A (red line), Case B (green line), Case C (blue line), Case D (black line) and Case E (yellow line). The cutting plane of the trace is a plane going through the origin with the elevation  $(90^\circ - \phi)$  of  $0^\circ$ ,  $30^\circ$ ,  $45^\circ$ ,  $56^\circ$ ,  $90^\circ$ , respectively. Due to the imperfect omnidirectional property of the output power, rotations in every plane leads to a unique pattern. In our experiments, we use the above-mentioned five trajectories to rotate the receiver.

The key advantage of the proposed scheme is that it is inherently high-efficient in the 3D space without the need for any active tuning or control. However, the output power may drop at certain angular positions (this is inevitable in any omnidirectional WPT system with a fixed supply voltage), which can be solved by using adaptive tuning methods either by adjusting the input voltage or by adjusting the effective load impedance at the receiver side. Note that the efficiency of the system will still be high even with a drop in the output power. Therefore, in certain applications it may be not even necessary to regulate it. For example, in a battery charging application, the battery may still be charged with a lower power level, but fully efficiently.

## IV. EXPERIMENTAL VERIFICATION

### A. The Experimental Setup

Next, we verify the proposed omnidirectional WPT system with novel toroidal helix coils. Fig. 11 shows the experimental setup. The coils are made from a Litz wire wrapped on a torus whose major and minor radii are 90 mm and 10 mm, respectively. In the experimental setup, the transmitter is placed in the  $xoy$  plane and is rotated around the center of the 3D Tx-Rp structure to realize receiver orientations described in Section II. When the Tx-Rp is rotated about  $y$  axis, the measurement results are marked as Cases A, B, C, and D, which correspond to the numerical results in Section II [see Fig. 10(b) for the illustration of corresponding

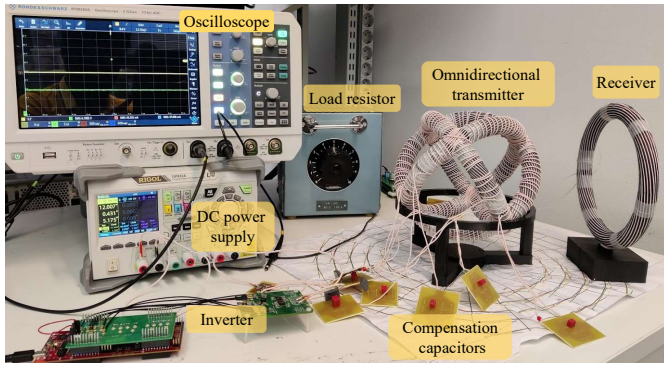


Fig. 11. The experimental setup.

receiver trajectories for different cases]. All the coils are tuned to the design frequency using low-loss Polypropylene film capacitors, and the experimental operational frequency is set to 578 kHz, which is slightly different from the design frequency due to the availability of tuning capacitors. For the power source, a full-bridge inverter is built using two Gallium Nitride half-bridges LMG5200. The load resistance is connected to the Rx coil through a diode rectifier. The receiver moves around the origin in the plane of  $xoy$  from  $\phi = 0^\circ$  to  $\phi = 360^\circ$ , with the fixed distance of Rx to the center 200 mm. The experimentally measured  $\gamma_{1,2,3}$  have been found to be ranging between 0.04 and 0.06 throughout all the Rx positions, which justifies the assumption  $\gamma_{1,2,3} = \gamma_0$  made during the theoretical analysis.

### B. Results against Receiver Misalignment

The experimental results of the output power and efficiency are shown in Fig. 12(a) and Fig. 12(b), respectively, for the five selected receiver trajectories. The efficiency is measured from the DC power sources to the DC load. From Fig. 12(b) we can observe that the measured DC-to-DC efficiency is relatively constant regardless of the Rx position. The slightly lower measured efficiency is due to the fact that only coil losses are considered in the numerical calculations while the measured one includes the losses in the inverter and the rectifier. We see that the output power profiles follow the theoretical curves of  $M_{\text{sum}}^2$  variations when the receiver position changes [see Fig. 10(b)]. Considering the selected five cases, Case D shows a relatively stable variation of output power. Case A has the highest output power fluctuations since at this Rx trajectory,

TABLE I  
MEASURED PARAMETERS OF THE WPT COILS

	Inductance ( $\mu\text{H}$ )	Resistance ( $\text{m}\Omega$ )	$Q$
Tx1	7.90	225	122
Tx2	8.00	220	126
Tx3	7.99	229	120
Rp1	108.68	657	582
Rp2	108.15	687	580
Rp3	109.09	678	603
Rx	106.7	680	595

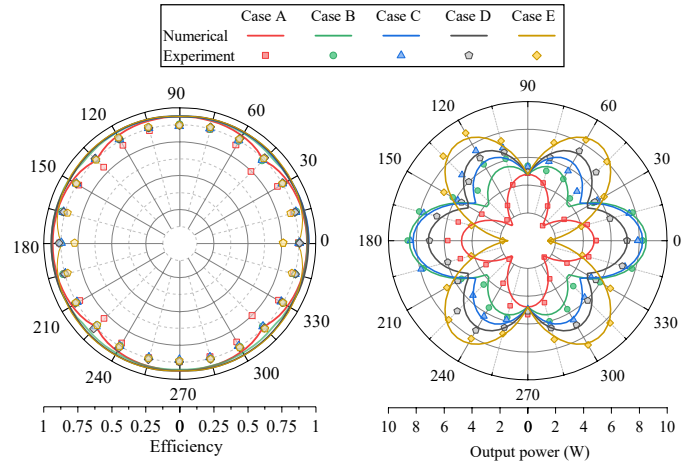


Fig. 12. (a) The efficiency of the proposed WPT system, and (b) the output power of the proposed WPT system, with respect to receiver position in different traces.

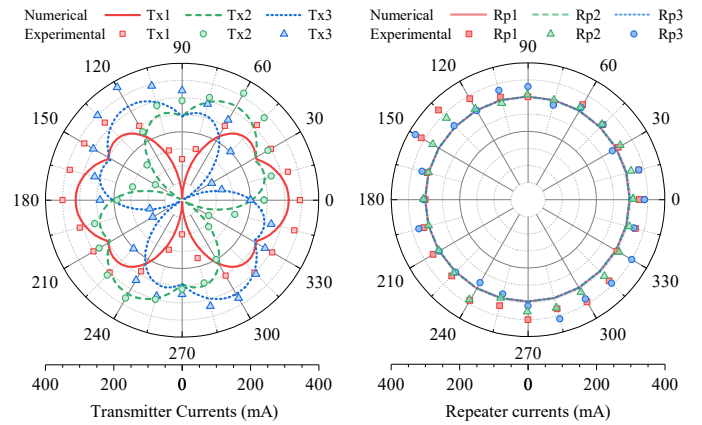


Fig. 13. (a) The Tx currents of the proposed WPT system under the condition of Case D; (b) The repeater currents of the proposed WPT system under the condition of Case D.

the pair Tx3-Rp3 is orthogonal to the Rx plane and does not contribute to the power transfer.

Since the stable performance of the output power is the best for Case D, we take it as an example to do further measurements. First, we confirm the self-tuning feature. The measured Tx and Rp currents for Case D are presented in Fig. 13. While the variations of Tx currents follow the mutual inductance profile, the Rp currents remain almost constant against the rotational angle of receiver. Therefore, it is apparent that the power flow from each Tx is self-adjusted depending on the mutual inductance between the repeater in the same power channel and the Rx. This self-tuning functionality ensures a very efficient power transfer in all directions.

Next, we rotate the receiver coil around its own vertical axis (indicated as “self-rotation” in Fig. 11). Unlike the previous receiver’s rotation around the Tx arrangement, here, the self-rotation of the receiver represents an application scenario with an angular misalignment. Fig. 14(a) shows the measured output power and efficiency where we define the self-rotation angle  $0^\circ$  when the Rx is aligned towards the center of the Tx

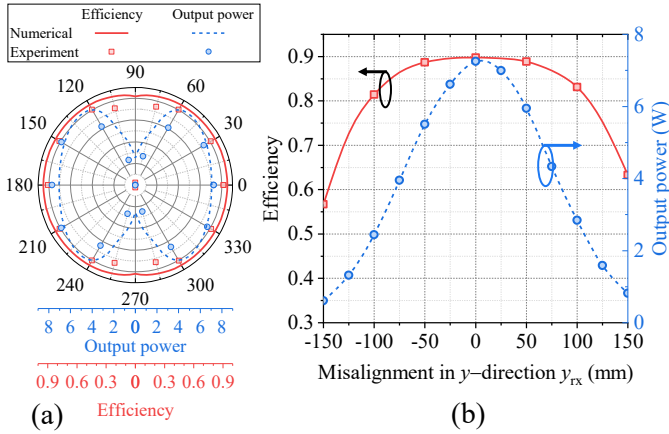


Fig. 14. (a) The output power and efficiency of the proposed WPT system when Rx rotates around its center, (b) The output power and efficiency of the proposed WPT system when Rx moves along  $y$ -axis.

sphere. It is worth to point out that at the angles  $90^\circ$  and  $270^\circ$  the output power drops sharply because the mutual inductance  $R_p$ - $R_x$  is at its minimum (here, the receiver is orthogonal to the nearest repeater). However, even with a such sharp drop, the efficiency is still maintained at a high level due to the self-tuning functionality of the proposed system. For the extreme angles of  $90^\circ$  and  $270^\circ$  the output power drops, however, a slight rotation from these angles restores the efficiency of the power transfer.

Another possible misalignment case is the receiver displacement in the  $y$  direction with the normal vector parallel to  $x$  axis. Fig. 14(b) shows the efficiency and output power in Case D for the fixed  $x$  coordinate 200 mm of the receiver that moves linearly along the  $y$  direction. Along this trajectory, the receiver is directly oriented to the center of the Tx sphere only at position  $y = 0$ , otherwise, its orientation is parallel to  $x$  axis. As we expect, symmetry of the efficiency and output power variations exists for positive and negative values of  $y$ . It can be observed that the efficiency drop is smaller than 3% for a 110 mm span of the receiver in  $y$ -directed displacement (i.e.,  $-55 \text{ mm} < y < 55 \text{ mm}$ ). Even with an extreme misalignment at 150 mm, the efficiency drop is only 35%. In practical applications, such extreme misalignment in the  $y$ -direction would not be expected. On the other hand, the output power profile shows a steeper drop with respect to  $y$ -misalignments due to the unavoidable mutual inductance drop. As discussed earlier, the drop in the output power with respect to receiver misalignment is inevitable in any omnidirectional WPT system, which can be compensated if needed by adjusting the supply voltage. The most important requirement is high efficiency of the WPT system over most of the possible locations and orientations of the receiver coil. The proposed WPT system clearly respects this requirement. Our results prove that high efficiency is achievable throughout all the Rx positions in space with realistic angular and displacement misalignments.

### C. Results with Multiple Receivers

As an extension, we have experimentally studied the performances of the proposed omnidirectional WPT with two receiver loads charging at the same time. To this end, an identical second receiver is placed together with the first one studied earlier. One receiver ( $R_{x1}$ ) is fixed at zero angular position, and the other receiver ( $R_{x2}$ ) is moved along the trajectory of Case D. The variation of total DC-to-DC efficiency and the output powers with respect to the angle of the second receiver are shown in Fig. 15 (note that the angles between  $0^\circ$  to  $60^\circ$  and  $300^\circ$  to  $360^\circ$  were not feasible due to the size restrictions of the coils). We can observe a couple of notable characteristics from the results. Firstly, the total DC-DC efficiency remains almost 90% regardless of the addition of the second receiver, or of its position. This is because the self-tuning capability of the proposed WPT system ensures that the input power from the source is self-tuning based on the power demand by the receivers. Secondly, the power received by the stationary receiver ( $R_{x1}$ ) remains stable if cross-coupling between two receivers is not very significant, i.e., except the positions of the moving receiver ( $R_{x2}$ ) over  $90^\circ$ . Thirdly, the power received by the moving receiver is the same as the stationary one when both receivers are placed at the opposite sides of the Tx structure (i.e., at  $180^\circ$  angle). However, when the position of  $R_{x2}$  is different from the opposite side of the Rx (e.g., at angles smaller  $150^\circ$  or larger than  $210^\circ$ ), the power received from  $R_{x2}$  is not very high. This is indeed expected because the equivalent magnetic field vector is oriented towards  $R_{x1}$ , as the current directions in  $R_p$  coils are optimized for the  $R_{x1}$  position, as discussed in [10]. In order to optimize the power flow for the both receivers, the Tx switching strategy needs to be optimized for both Rx positions. For example, time division multiplexing of magnetic field vector could be used for such optimization.

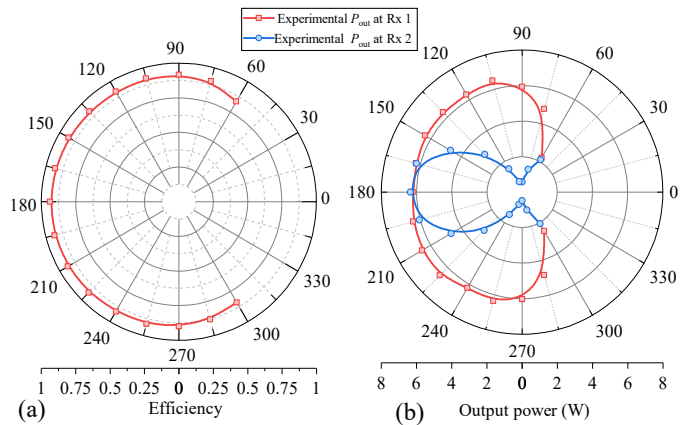


Fig. 15. The performance variation with respect to the angle of the second receiver when one receiver is fixed at zero angular position, and the other receiver is moved along the trajectory of Case D: (a) total DC-to-DC efficiency and (a) the output powers.

Next, the experimental study is further continued with two receivers where the two receivers are kept at the opposite sides of the Tx (i.e.,  $180^\circ$  separation between the two Rx) rotated around the Tx structure. We can observe from the

results in Fig. 16 that the power received at both receivers follows the theoretical power profile, and the total efficiency remains stable at around 90% regardless of the rotation angle. Therefore, it is clear that the proposed structure is applicable to omnidirectional WPT with multiple Rxs. It should be noted that the optimization of such WPT systems with multiple Rxs needs to be further analysed, which is beyond the scope of this paper.

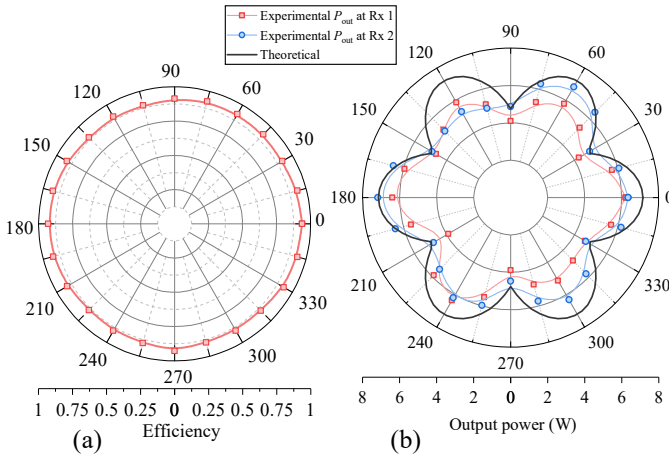


Fig. 16. The performance variation with respect to the receiver position when the both receivers are rotated together around the Tx with a  $180^\circ$  angle between two Rxs.

#### D. Load Impedance Variations

Next, we verify the performance characteristics through experiments with different load resistances. We use the load resistances of  $10\ \Omega$ ,  $20\ \Omega$ ,  $47\ \Omega$ ,  $94\ \Omega$ ,  $470\ \Omega$ , and  $1000\ \Omega$  and carry out the same testing procedure for Case D, measuring the efficiency and output power, see Fig. 17. The experimental results generally agree well with the theoretical results with a slight deviation due to experimental disparities discussed above. For the efficiency and output power, the optimal resistances of the load are almost the same as the ones that we derived in Section II-B (around  $20\ \Omega$ ). The deviation of the experimental output power at low load resistance values ( $10\ \Omega$ ) is mainly attributed to higher losses in the rectifier circuit.

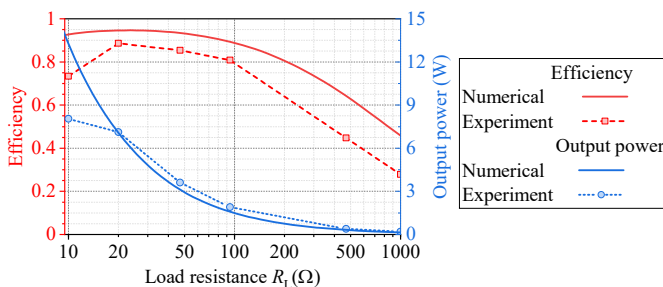


Fig. 17. The output power and efficiency of the proposed WPT system when the load changes.

## V. CONCLUSION

This paper presents a high-efficiency omnidirectional wireless power transfer (WPT) system based on an original double toroidal helix coil structure. Three pairs of orthogonal toroidal helix coils – three transmitters (Tx) and three repeaters (Rps) – form three independent *power channels*. The proposed scheme enables self-tuning power flow in each *power channel* depending on the mutual coupling between each channel and the receiver (Rx) coil, resulting in high efficiency for almost all Rx positions and orientations at a suitable distance from the transmitters. The prime requirement to achieve self-tuning power flow and high efficiency is that both Tx-Rp and Rp-Rx coil pairs should be strongly coupled while the coupling between Tx-Rx should be as minimum as possible. To this end, we propose toroidal helix coils that can create two types of orthogonal magnetic fields – in poloidal directions and toroidal directions. Then the coupling between Tx-Rp coil pair is predominantly due to toroidal field coupling and the coupling between Rp-Rx coil pair is predominantly due to poloidal field coupling. Most importantly, strengths of the toroidal and poloidal fields can be independently engineered by choosing proper design parameters for poloidal and toroidal numbers of turns. A design study is presented together with a design procedure. Experimental results show that the power transfer efficiency remains around 90% over almost full range of receiver positions at transfer distance of 200 mm. In addition, the different cases of misalignment including receiver's self-rotation and displacement have been studied. The efficiency experiences low variation for the receiver's rotating around its axis and lateral displacement. Finally, the load impedance impact for efficiency and output power is verified. The proposed WPT system appears to be promising for various wireless power transfer systems, for example, a study of the proposed coil type with different compensation topologies would be an interesting future research direction.

## REFERENCES

- [1] W. Lin and R. W. Ziolkowski, "A circularly polarized wireless power transfer system for internet-of-things (IoT) applications," in *2020 4th Australian Microwave Symposium (AMS)*. IEEE, 2020, pp. 1–2.
- [2] Z. Zhang and B. Zhang, "Omnidirectional and efficient wireless power transfer system for logistic robots," *IEEE Access*, vol. 8, pp. 13 683–13 693, 2020.
- [3] M. Kim, D.-M. Joo, and B. K. Lee, "Design and control of inductive power transfer system for electric vehicles considering wide variation of output voltage and coupling coefficient," *IEEE Transactions on Power Electronics*, vol. 34, no. 2, pp. 1197–1208, 2018.
- [4] A. N. Abdulfattah, C. C. Tsimenidis, B. Z. Al-Jewad, and A. Yakovlev, "Performance analysis of mics-based RF wireless power transfer system for implantable medical devices," *IEEE Access*, vol. 7, pp. 11 775–11 784, 2019.
- [5] W. M. Ng, C. Zhang, D. Lin, and S. R. Hui, "Two-and three-dimensional omnidirectional wireless power transfer," *IEEE Transactions on Power Electronics*, vol. 29, no. 9, pp. 4470–4474, 2014.
- [6] C. Zhang, D. Lin, and S. Hui, "Basic control principles of omnidirectional wireless power transfer," *IEEE Transactions on Power Electronics*, vol. 31, no. 7, pp. 5215–5227, 2015.
- [7] B. H. Choi, E. S. Lee, Y. H. Sohn, G. C. Jang, and C. T. Rim, "Six degrees of freedom mobile inductive power transfer by crossed dipole Tx and Rx coils," *IEEE Transactions on Power Electronics*, vol. 31, no. 4, pp. 3252–3272, 2015.
- [8] Z. Dai, Z. Fang, H. Huang, Y. He, and J. Wang, "Selective omnidirectional magnetic resonant coupling wireless power transfer with multiple-receiver system," *IEEE Access*, vol. 6, pp. 19 287–19 294, 2018.

- [9] W. Han, K. T. Chau, C. Jiang, W. Liu, and W. H. Lam, "Design and analysis of quasi-omnidirectional dynamic wireless power transfer for fly-and-charge," *IEEE Transactions on Magnetics*, vol. 55, no. 7, pp. 1–9, 2019.
- [10] X. Dang, P. Jayathurathnage, F. Liu, C. Simovski, and S. A. Tretyakov, "Omnidirectional wireless power transfer with automatic power flow control," *arXiv preprint arXiv:1909.10175*, 2019.
- [11] J. Li, Y. Yang, H. Yan, C. Liu, L. Dong, and G. Wang, "Quasi-omnidirectional wireless power transfer for a sensor system," *IEEE Sensors Journal*, vol. 20, no. 11, pp. 6148–6159, 2020.
- [12] W. Tang, Q. Zhu, J. Yang, D. Song, M. Su, and R. Zou, "Simultaneous 3-d wireless power transfer to multiple moving devices with different power demands," *IEEE Transactions on Power Electronics*, vol. 35, no. 5, pp. 4533–4546, 2020.
- [13] O. Jonah, S. V. Georgakopoulos, and M. M. Tentzeris, "Orientation insensitive power transfer by magnetic resonance for mobile devices," in *2013 IEEE Wireless Power Transfer (WPT)*. IEEE, 2013, pp. 5–8.
- [14] L. Tan, R. Zhong, Z. Tang, T. Huang, X. Huang, T. Meng, X. Zhai, C. Wang, Y. Xu, and Q. Yang, "Power stability optimization design of three-dimensional wireless power transmission system in multi-load application scenarios," *IEEE Access*, vol. 8, pp. 91 843–91 854, 2020.
- [15] D. Lin, C. Zhang, and S. R. Hui, "Mathematic analysis of omnidirectional wireless power transfer—part-II three-dimensional systems," *IEEE Transactions on Power Electronics*, vol. 32, no. 1, pp. 613–624, 2016.
- [16] J. Lu, G. Zhu, D. Lin, Y. Zhang, J. Jiang, and C. C. Mi, "Unified load-independent zpa analysis and design in CC and CV modes of higher order resonant circuits for wpt systems," *IEEE Transactions on Transportation Electrification*, vol. 5, no. 4, pp. 977–987, 2019.
- [17] D. Kim and D. Ahn, "Self-tuning LCC inverter using pwm-controlled switched capacitor for inductive wireless power transfer," *IEEE Transactions on Industrial Electronics*, vol. 66, no. 5, pp. 3983–3992, 2019.
- [18] H. Han, Z. Mao, Q. Zhu, M. Su, and A. P. Hu, "A 3D wireless charging cylinder with stable rotating magnetic field for multi-load application," *IEEE Access*, vol. 7, pp. 35 981–35 997, 2019.
- [19] J. M. Arteaga, S. Aldhaher, G. Kkelis, C. Kwan, D. C. Yates, and P. D. Mitcheson, "Dynamic capabilities of multi-MHz inductive power transfer systems demonstrated with batteryless drones," *IEEE Transactions on Power Electronics*, vol. 34, no. 6, pp. 5093–5104, 2019.
- [20] X. Dang, P. Jayathurathnage, S. A. Tretyakov, and C. R. Simovski, "Self-tuning multi-transmitter wireless power transfer to freely positioned receivers," *IEEE Access*, vol. 8, pp. 119 940–119 950, 2020.
- [21] S. Babic, F. Sirois, C. Akyel, and C. Girardi, "Mutual inductance calculation between circular filaments arbitrarily positioned in space: Alternative to grover's formula," *IEEE transactions on magnetics*, vol. 46, no. 9, pp. 3591–3600, 2010.
- [22] J. P. K. Sampath, A. Alphones, and H. Shimasaki, "Coil design guidelines for high efficiency of wireless power transfer," in *2016 IEEE Region 10 Conference (TENCON)*, 2016, pp. 726–729.